Converting genetic network oscillations into somite spatial patterns

K. I. Mazzitello,[1] C. M. Arizmendi,[2] and H. G. E. Hentschel[3]
[1]*CONICET-Facultad de Ingeniería, Universidad Nacional de Mar del Plata, Argentina*
[2]*Facultad de Ingeniería, Universidad Nacional de Mar del Plata, Argentina*
[3]*Department of Physics, Emory University, Atlanta, Georgia 30322, USA*
(Received 14 April 2008; revised manuscript received 1 July 2008; published 14 August 2008)

The segmentation of vertebrate embryos, a process known as somitogenesis, depends on a complex genetic network that generates highly dynamic gene expression in an oscillatory manner. A recent proposal for the mechanism underlying these oscillations involves negative-feedback regulation at transcriptional translational levels, also known as the "delay model" [J. Lewis Curr. Biol. **13**, 1398 (2003)]. In addition, in the zebrafish a longitudinal positional information signal in the form of an Fgf8 gradient constitutes a determination front that could be used to transform these coupled intracellular temporal oscillations into the observed spatial periodicity of somites. Here we consider an extension of the delay model by taking into account the interaction of the oscillation clock with the determination front. Comparison is made with the known properties of somite formation in the zebrafish embryo. We also show that the model can mimic the anomalies formed when progression of the determination wave front is perturbed and make an experimental prediction that can be used to test the model.

DOI: 10.1103/PhysRevE.78.021906 PACS number(s): 87.17.Pq, 87.17.Aa, 87.18.Cf, 87.17.Ee

I. INTRODUCTION

Genetic networks can create complex temporal distributions of intracellular proteins in cells, and it is these changes in cells (the genotype) that ultimately results in multicellular morphogenesis in which complex spatial and temporal distributions of cells are observed (the phenotype). A great deal of biological work has been expended in identifying these intracellular genetic networks, but how they ultimately lead to morphogenesis remains to a large degree unknown. One very-well-studied case biologically is, however, the genetic network involved in somite formation (the embryonic repeated backbone and associated musculature structure in vertebrates). Many of the elements of this genetic network have been identified, and its oscillatory dynamics suggests that an intracellular clock mechanism is involved in somitogenesis. Such a somitogenesis clock has been identified in chick, mouse, zebrafish, and frog, which results in oscillatory gene expression of several proteins in the presomitic mesoderm. Two major questions are therefore how such somitogenesis clock oscillations are generated and how they regulate segmentation. The intracellular oscillations are by now well understood and are described below, while how they may interact to create spatial structure is the subject of this paper.

Genetic oscillators play an important role in various biological processes. Probably the best known are the circadian clocks which permit organisms to anticipate the daily changes of environmental conditions. Less known but not less important is the segmentation clock [1,2], which is thought to drive the periodic and sequential segmentation of the vertebrate embryo along its anterior-posterior axis into blocks of cells called somites, the precursors of axial bone and muscle. This clock comprises a multicellular genetic network of oscillators located within the presomitic mesoderm (PSM).

Because of the crucial nature of segmentation in multicellular development, several models have been proposed to explain such periodic spatial structures [1,3–7]. The clock and wave-front model proposed by Cooke and Zeeman in 1976 [2] is perhaps best known, but others include Meinhardt's reaction diffusion model [8]; and Stern and coworker's cell cycle model [9].

The clock and wave-front model postulates the existence of a longitudinal positional information gradient down the axis of vertebrate embryos. This gradient interacts with the cellular oscillator, stopping the oscillations and producing a rapid change in locomotory and adhesive behavior of cells when they form somites. The oscillation in the PSM is the somite clock, and the moving interfaces at the anterior end of the PSM where the positional information reaches a critical value is called the wave front. It is the interaction between the clock phase and the positional information that controls somitogenesis.

Recent prevailing models of somitogenesis [10,11] are new versions of the clock and wave-front model involving groups of cells within the presomitic mesoderm (the segmental plate) coalescing under the control of a slow-moving wave front (in the anterior-to-posterior direction) and an intracellular oscillatory cycle within the cells [3–6,10,12–14]. Very recently, a model for the segmentation clock applied to mouse somitogenesis has been published [15]. In such clock and wave-front models, the state of the cells in the cycle dictates what the cells should do when the wave front triggers them. The production of segmental boundaries occurs when cells in a permissive phase of the clock cycle encounter a maturation wave front progressing caudally in the PSM. As a result, segments are formed in a rostral-to-caudal (head-to-tail) fashion at a temporal frequency defined by the clock and a spacing defined by the speed of wave-front progression in the PSM. The result is repeated "slicing" of the presomitic mesoderm into somite-sized units (Fig. 1).

Following these assumptions, we have therefore constructed a deterministic one-dimensional model and compare the resulting spatial patterning with the somites for zebrafish embryo. We use in our model a recent proposal for the

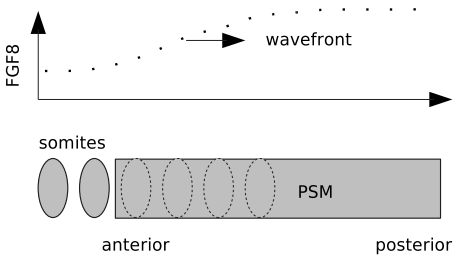

FIG. 1. An schematic illustration of somite formation within the clock and wave-front model. Gene and gene product concentrations in the cells of PSM experience temporal oscillations. In the top part of the diagram, the positional information wave front is illustrated together with the position of the determination front which we assume represents the position at which the Fgf8 concentration gradient falls below a critical value. The somites form in an anterior to posterior order as the wave front advances from head to tail.

mechanism producing the intracellular oscillations as due to delays in the synthesis of mRNA focusing specifically on the zebrafish genes *her*1 and *her*7 and their gene products the protein molecules Her1 and Her7 [12]. The position of the wave front was shown to be defined by the concentration of the secreted factor Fgf8 whose mRNA is expressed in a graded fashion in the caudal PSM [14]. In our model the signal created by the Fgf8 concentration interacts with the clock phase (the intracellular concentration of a gene protein), leading to cell differentiation and somite formation. At low Fgf8 concentration, cell arrangement becomes more compact and the epithelialization process underlying somite formation begins. Similar results are obtained with our model; somite formation begins when the interaction of the determination front is done through *her*1 or *her*7 gene or gene product, while the gene oscillation characteristic of the immature PSM is sustained when the interaction is through *deltaC* gene or gene product.

Recently, some attention has been paid to genetic networks in physics journals: on small networks like the mixed feedback loop [16] or toggle switch [17], on synthetic genetic networks [18], and an interesting study of the relation between the quality of oscillations of the genetic networks and stochastic time delays [19]. In this work the interaction of a genetic clock with a spatial genetic signal producing a spatial pattern is studied.

The paper is therefore written with the following structure: Section II is devoted to the description of the proposed model and contains the results derived from it. In Sec. III, we describe our proposal for the interaction of the Fgf8 gradient with the clock phase of the genetic network as a *her*1 repressor. The transcription in the synthesis of mRNA is essentially a noisy process and is considered for haploid cells in the Sec. IV. In Sec. V, we study the effect of a local perturbation of the Fgf8 wave front on the spatial pattern of somites. Finally a conclusion and discussion are presented in Sec. VI.

II. MODEL FOR SOMITE FORMATION

Oscillations in biological systems are typically generated by negative-feedback loops [20]. The oscillator might be some molecule that, with a delay, directly or indirectly inhibits its own production or activation. Recent papers have identified *her*1 and *her*7 as a pair of genes in the zebrafish that jointly satisfy all these conditions to be central components of the oscillator. Their mRNA concentrations normally oscillate in synchrony in the PSM, matching the periodicity and phase of the gene *deltaC*, as though the mRNA levels of all three genes are coordinately regulated [6]. When chromosomal deletion [1] or morpholino injections reduce the levels of *her*1 and *her*7 or their gene products, the *deltaC* expression in the PSM also fails to oscillate and the physical pattern of somite segmentation becomes grossly irregular. Similar but weaker effects are produced when morpholino knockdown of *her*1 by itself [1,5,6]. In addition, it is known that both genes are positively regulated by Notch signaling [6,7] between cells (see below), and, most importantly, they appear to negatively regulate their own expression [5,6].

Although the simplest possibility would be a feedback loop in which Her1 or Her7 protein (we will use the notation that *her* refers to gene mRNA while Her corresponds to the gene product protein) directly binds to the regulatory DNA of its own gene to inhibit transcription, it has been shown that it is impossible to generate sustained oscillations in this way [12]. Nevertheless, sustained oscillations can be obtained via a negative delayed feedback [19,21], simply by taking account of the delays involved in the synthesis of mRNA and proteins: the time between initiation of transcription and arrival of the mature mRNA molecule in the cytoplasm, T_m, and the delay, T_p, between the initiation of translation and the emergence complete functional protein molecule.

In order that cellular oscillations can couple in the multicellular system leading to the possibility of synchronous dynamics, intracellular oscillations by themselves are not enough and some cell-cell coupling mechanism is required. This is supplied by the Notch pathway. Thus in the Notch pathway mutants in which this coupling is missing the neighboring cells are observed in a random assortment of phases. On the other hand, the oscillators in neighboring cells must normally be capable to some extent of influencing one another, and when the Notch pathway functions, synchrony can occur.

In other respects, however, we shall try and keep the known biology, including a clock set by coupled intracellular genetic networks using Notch signaling to couple the networks in the PSM [12]; and in order to consider a genetic network explanation for the FGF signaling effect observed biologically, we have included in our simulations self-repression of *her*1 through formation of Her1-Her13.2 heterodimer complex.

One key approximation in our simulations will be to keep the model one dimensional. Although the PSM is in reality a three-dimensional structure and a mediolateral spread of expression waves has been described in chick [22], for the purposes of this study only the dominant variations along the anteroposterior axis will be considered.

The model thus consists initially of a linear array of N_{start} cells that represents the starting size of the PSM with intracellular oscillators driven by the *her*1 and *her*7 genes and their associated gene product proteins. The oscillations be-

tween nearest-neighbor cells are coupled and synchronized via Notch signaling [23,24]. The cell-cell communication produced by means of the *deltaC* gene product Notch crossing the cell membrane wall. In each cell in the array the gene mRNA concentrations m_k for the genes $k \equiv her1$, *her*7, *deltaC* and their associated gene products the protein concentrations p_k obey the sets of coupled kinetic equations (see [12])

$$\frac{dp_k^i}{dt}(t) = am_k^i(t - T_{p_k}) - bp_k^i(t),$$

$$\frac{dm_k^i}{dt}(t) = \frac{1}{nn}\sum_{i'=1}^{nn} f_k(p_{her1}^i(t - T_{m_k}), p_{her7}^i(t - T_{m_k}), p_{deltaC}^{i'}(t - T_{m_k})) - cm_k^i(t). \quad (1)$$

Here the symbol i denotes the cell position in the linear array; i' goes from 1 to nn the number of near-neighbor cells of i (nn can be 1 if i is at an end or otherwise 2), T_{m_k} is the delay time from initiation of transcription to export of the mature mRNA m_k into the cytosol, T_{p_k} is the delay between the initiation of translation and the emergence of the complete protein molecule p_k, a represents the protein p_k synthesis rate per mRNA molecule, b is the rate of protein p_k degradation, and c is the rate of mRNA m_k degradation, while the function f_k represents the rate of production of new mRNA molecules m_k.

In order to reproduce oscillatory transcription with minimum regulations we take into account only essential regulations. To represent the action of protein products of *her*1 and *her*7, regulation by homodimers of Her is not essential for the cyclic transcription. Experimental observation supports the exclusion of their involvement [25]. Somite segmentation and clock gene expression is disrupted in the absence of either Her1 or Her7, suggesting that the Her1/Her7 heterodimer plays the central role [26]. For the *delta* expression, consideration of Her-dependent repression is sufficient and another regulation term is not essential. Furthermore, there is no experimental evidence that *delta* is under the control of self-regulation in addition to Her-dependent repression [23,27].

In order to represent the action of protein products of *her*1 and *her*7 that combine as a heterodimer to inhibit *her*1 and *her*7 expression and the positive regulation due to activated notch, f_k is assumed to be a decreasing function of the amount of proteins p_{her1}, p_{her7}, and an increasing function of the concentration of p_{deltaC} [28]. Thus, $f_{k=her1/7}$ and $f_{k=deltaC}$ are given by the Michaelis-Menten kinetics [12]

$$f_{her1/7}(p_{her1}^i(t'), p_{her7}^i(t'), p_{deltaC}^{i'}(t')) = K_{her1/7}\frac{\phi_{deltaC}^{i'}(t')}{1 + \phi_{deltaC}^{i'}(t')}\frac{1}{1 + \phi_{her1}^i(t')\phi_{her7}^i(t')},$$

$$f_{deltaC}(p_{her1}^i(t'), p_{her7}^i(t'), p_{deltaC}^{i'}(t')) = K_{deltaC}\frac{1}{1 + \phi_{her1}^i(t')\phi_{her7}^i(t')}, \quad (2)$$

where we used the notation $t' = t - T_{m_k}$ and $\phi_k^i(t) = p_k^i(t)/p_k^{crit}$. $p_{her1/7}^{crit}$ is the critical number of molecules of Her1 or Her7 protein per cell, for inhibition of transcription, while p_{deltaC}^{crit} represents the critical number of Notch molecules required for activation of transcription. The mRNA concentrations for the kind different of genes decrease when the Her1/7 protein concentration are larger than their critical values $p_{her1/7}^{crit}$ or when the DeltaC protein Notch concentration is below its critical value p_{deltaC}^{crit}.

The concentrations of intercellular signaling molecules in the cells are coupled between the nearest-neighbor nn cells by means of the function f_k through the DeltaC protein Notch concentration of their neighboring cells $p_{deltaC}^{i'}(t - T_{m_k})$, as can be seen in Eq. (2). The mRNA and protein oscillations can occur without interactions between neighbor cells, because the delays that take part in feedback loops are intracellular. The interactions through f_k connecting neighbor cells are, however, crucial as they result in synchronous in-phase oscillations in the linear array representing the PSM as a whole to occur.

The concentrations of both protein and mRNA molecules, p_k and m_k, are set equal to zero initially in all N_{start} cells of the linear array. The temporal evolution of p_k and m_k are calculated with Eqs. (1) and (2), for all molecules of the linear array. To see whether *her*1 and/or *her*7 could generate oscillations, the parameters a, b, c, K, p_k^{crit}, T_{m_k}, and T_{p_k} were estimated by Lewis [12] using biological data. The ranges estimated for the intracellular delays are $10.2\ \text{min} < T_{m_{her1}} < 31.5\ \text{min}$, $T_{p_{her1}} \cong 2.8\ \text{min}$, $5.9\ \text{min} < T_{m_{her7}} < 20.1\ \text{min}$, and $T_{p_{her7}} \cong 1.7\ \text{min}$, and the corresponding ranges for the delays in the cell-cell signaling pathway are, $16\ \text{min} < T_{m_{deltaC}} < 68\ \text{min}$ and $T_{p_{deltaC}} \cong 5.5\ \text{min}$. Plausible values of the constants involved in Eqs. (1) and (2) reported for mRNA and proteins in eukaryotic cells are $a = 4.5$ protein molecules per mRNA molecule per minute [29]; $b = c = 0.23$ molecules per minute, corresponding to protein and mRNA half-lives of 3 min [30,31]; $1 \leqslant K_k \leqslant 200\ \text{min}^{-1}$ [32] (we use in our simulations $K_k = 33$ mRNA molecules per diploid cell per minute, corresponding to 1000 transcripts per hour per gene copy in the absence of inhibition [29]); $p_{her1/7}^{crit} = 40$ molecules, corresponding to a critical concentration of $\sim 10^{-9}\ M$ within a 5-μm-diameter cell nucleus and in the same way $p_{deltaC}^{crit} = 1000$.

Concentrations of mRNA molecules of gene *her*1 and its associated gene product protein Her1 as a function of time for any cell of the PSM before somite formation begins are shown in Fig. 2. Sustained oscillations of both concentrations are obtained for the values of parameters specified in the figure caption. The period obtained with these parameter values is in good agreement with the observed period of 30 min for the zebrafish somite oscillator at 28 °C.

We suppose at time $t = 0$ all the cells in the starting PSM to be oscillating in phase, and therefore we begin with the

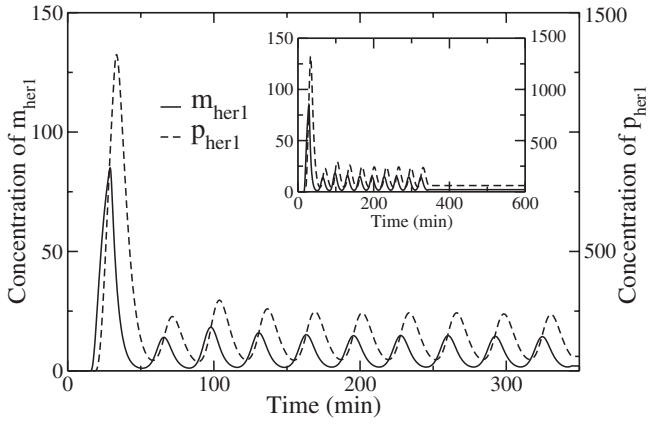

FIG. 2. Concentrations of mRNA molecules (number of molecules per cell) of gene *her*1 and its associated gene product protein Her1 as a function of time for any cell of the linear array, including the boundary cells. Sustained oscillations of both concentrations are obtained for the following values of parameters involved in Eqs. (1) and (2): $a=4.5$, $b=0.23$, $c=0.23$, $K_k=33$, $p^{crit}_{her1/7}=40$, $p^{crit}_{delta}=1000$, $T_{m_{her1}}=10.2$, $T_{m_{her7}}=5.9$, $T_{m_{deltaC}}=16$, $T_{p_{her1}}=2.8$, $T_{p_{her7}}=1.7$, and $T_{p_{deltaC}}=5.5$ min. (Inset) The oscillations are stopped when the corresponding cell is reached by the somitogenesis wave front. The concentrations of protein and mRNA molecules of genes *her*7 and *deltaC* have a similar behavior as the concentrations of m_{her1} and p_{her1} shown in this figure.

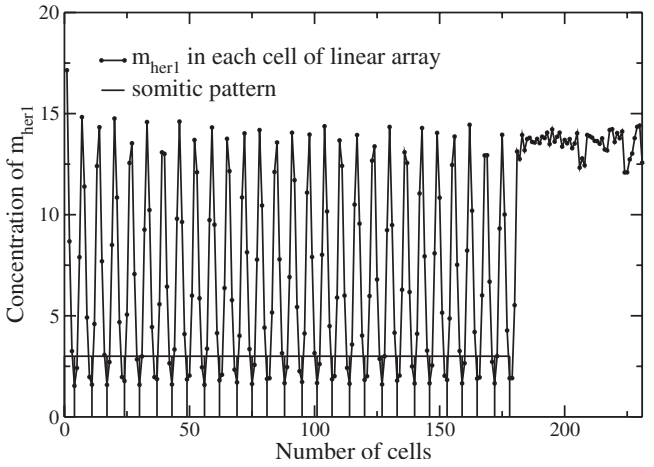

FIG. 3. Concentration of mRNA molecules (number of molecules per cell) of gene *her*1 as a function of cell number in the somites. The concentrations were calculated using Eqs. (1) and (2) and using the same parameter values as in the Fig. 2 (see caption). The concentration of m_{her1} belonging to cells that were reached by the wave front was frozen. In our simulation the wave front advances at a speed of one cell every 5 min. We see the simulation at time $t=900$ min at the end of somitogenesis in the zebrafish. At $t=900$ min, 28 somites have formed. All other concentrations of protein and mRNA molecules in the cells (namely, p_k with $k=$Her1, Her7, Notch and m_k with $k=$*her*7, *deltaC*) have the same qualitative behavior as the concentration of m_{her1}.

linear array of N_{start} cells and integrate the Eqs. (1) for the time necessary to obtain coherent synchronous oscillations.

The growth of the PSM is assumed to be produced by mitosis experienced by the last cells at the posterior end of the linear array. During the mitosis process the transcription and translation of genes are arrested [33] and cell division lasts at least 15 min [34]. In order to simulate these experimental features during the division we assume that the delay times are doubled and the synthesis rate of mRNAs and proteins is set to the halves. We calculate the rate of end cell division according to measured growth rates [35] of one cell every 5 min. Thus, it generates sequentially along the anteroposterior axis the necessary cells for forming the future segments of the embryo: the somites that are created at the anterior portion of the PSM; see Fig. 1. In our simulations, once the initial PSM has been obtained as a group of cells oscillating in phase, the caudal motion of the wave front starts. The wave-front velocity is given by the PSM growth rate of one cell every 5 min. We assume that the wave front interacts with cells by stopping the oscillations (see inset of Fig. 2). This effect may be obtained by freezing different sets of gene and gene product concentrations at their values when they meet the wave front, leaving the others to continue oscillating. The sets that accomplish this effect when freezed may be any gene or gene product of *her*1/7 or any combination of them. The gene oscillation is not stopped if the gene or gene product frozen are those of *deltaC* because the cell oscillation may be sustained without the Notch pathway communication in this model, as was shown experimentally in [36]. An ansatz for the interaction of wave front with oscillating genes is given in the section below. The observed spatial shift in the phases of different cells is thus obtained by the wave front catching different phases when passing through different cells, a biological implementation of the clock and wave-front model. We start with a PSM of 50 cells with a growth rate and a wave-front velocity of one cell every 5 min. We consider that the 20 last cells at the posterior end can experience mitosis. A wave front advancing at a rate of 1 cell/5 min creates a spatial wavelength of six to seven cells (Fig. 3). These six to seven cells form a somite, with a differentiated structure between the anterior and posterior portions of each somite. What the process is of cell differentiation after the cell meets the wave front is beyond the scope of this paper. When the simulation finishes in the time $t=900$ min, we find that 28 somite pairs have been created (Fig. 3). The wave front sweeps 180 cells and the posterior cells continue oscillating out of phase due to mitosis.

III. INTERACTION OF FGF8 GRADIENT WITH THE CLOCK PHASE

Recently, it has been shown that FGF signaling upregulates a basic helix loop-helix transcription factor, Her13.2, which maintains the oscillation of the Notch signals in both the tailbud and PSM [37]. It has been recently proposed that Hes6-related hairy/Enhancer of split-related gene, *her*13.2, links FGF signaling to the Notch-regulated oscillation machinery in zebrafish [38]. Her13.2 can act as a transcriptional repression with Her1, and enhancement of *her*1 repression by Her13.2 may be required for the periodical repression of *her*1 in the posterior PSM. Experimental results demonstrate that Her13.2 may enhance the self-repression of

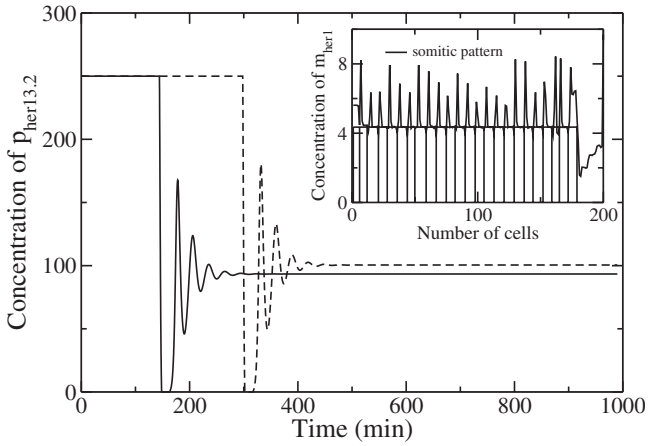

FIG. 4. Concentrations of protein molecules (number of molecules per cell) of gene *her*13.2 as a function of time for two different cells of the linear array. It is assumed that $p^i_{her13.2}(t)=250$ molecules for all cell i of the linear array until the wave front arrives at the time t_i, which depends on the cell i. Then, $p^i_{her13.2}(t)$ is obtained from the condition $m^i_{her1}(t)=m^i_{her1}(t_i)$ for $t \geqslant t_i$ denominated "freezing effect." We take $k_k=200$, $p^{crit}_{deltaC}=40$, and the other parameter values as in Fig. 2. (Inset) Concentration of mRNA molecules of gene *her*1 as a function of cell number in the somites. m_{her1} forms a presomitic pattern similar to the pattern obtained in Sec. II.

*her*1 presumably through formation of Her1-Her13.2 heterodimer complex [38]. In order to consider this result we propose in our model an additional repressive term in f_{her1}:

$$f_{her1}(p^i_{her1}(t'),p^i_{her7}(t'),p^{i'}_{deltaC}(t')) = K_{her1}\frac{\phi^{i'}_{deltaC}(t')}{1+\phi^{i'}_{deltaC}(t')}\frac{1}{1+\phi^i_{her1}(t')\phi^i_{her7}(t')} \frac{1}{1+\phi^i_{her1}(t')\phi^i_{her13.2}(t')}, \quad (3)$$

where $\phi^i_{her13.2}(t')=p^i_{her13.2}/p^{crit}_{her13.2}$ and $p^{crit}_{her13.2}$ is the critical number of molecules of Her13.2 protein per cell, for inhibition of transcription. All other variables were defined in the previous section. Thus, the temporal evolution of p_{her1} and m_{her1} for every cell in the array are calculated with Eqs. (1) and (3), while the temporal evolution of $p_{her7/deltaC}$ and $m_{her7/deltaC}$ for every cell in the array is calculated using Eqs. (1) and (2). The concentration of protein Her13.2, $p_{her13.2}$, is assumed to be high in posterior PSM before the arrival of the wave front according to previous experimental results [30]. The "freezing effect" proposed in the previous section means that the interaction of the wave front with cell i is supposed to fix $m^i_{her1}(t)$—that is, $m^i_{her1}(t)=m^i_{her1}(t_i)$ for all $t \geqslant t_i$, where t_i is the time of the passing of the wave front through the cell i. $p^i_{her13.2}(t)$ is obtained from the previous condition, for $t \geqslant t_i$. Whenever this condition results in a $p^i_{her13.2}(t)$ beyond the specified limits, it is forced to the nearest limit. In this case the freezing effect is not fulfilled, and $m^i_{her1}(t)$ are calculated with Eqs. (1) and (3). Figure 4 shows $p_{her13.2}$ as a function of time for different cells. In Fig. 4 it can be seen that there is a jump in protein concentration whenever the wave front passes through the cell, implying that the Her13.2 protein concentration is high in posterior PSM and drops in anterior PSM, agreeing with the experimental results. We think that the overdamped oscillations in $p_{her13.2}$ occurring at a short period of time until a stationary state is reached may be produced because we force abruptly the freezing effect in our model. The inset in the Fig. 4 shows the somitic pattern obtained considering the additional repressive term in f_{her1}. It is similar to the pattern obtained by the simple method of the wave front stopping the oscillations shown in Fig. 3.

IV. STOCHASTIC MODEL

Our simulations above assumed that no noise was present in the cells during transcription and translation, but as Lewis has pointed out, the transcription step involved in protein synthesis is essentially a stochastic process because of the small number of molecules involved in the cell [39]: A DNA molecule can randomly have a Her1, Her7, or Delta Notch dimer bound to its regulatory site. When such a dimer does bind, transcription is forbidden, whereas if no protein is bound at a regulation site of the DNA molecule, transcription occurs at the possible maximal rate.

The stochastic model for haploid cells is then constructed by taking the deterministic one-dimensional model and considering the possible states (bound and dissociated) of all regulatory sites of the *her*1, *her*7, and *deltaC* genes as stochastic variables [12]. The protein and mRNA concentrations are given by Eqs. (1) as in the deterministic case, but the functions f_k now describe a stochastic process and are therefore modified to

$$f_{her1/7}(p^i_{her1}(t'),p^i_{her7}(t'),p^{i'}_{delta}(t')) = K_{her1/7}\xi^i_{her1/7}(t')[1-\eta^{i'}_{her1/7}(t')],$$

$$f_{deltaC}(p^i_{her1}(t'),p^i_{her7}(t'),p^{i'}_{delta}(t')) = K_{deltaC}\xi^i_{deltaC}(t'), \quad (4)$$

where the functions $\xi_{her1/7}$, $\eta_{her1/7}$, and ξ_{deltaC} are random variables taking a value 1 when no protein is bound at the regulatory site and 0 when it is bound, with probabilities that depend on protein concentrations $p_k(t')$ in the cell i and in its neighbor cell i', at time $t'=t-T_{m_k}$ when synthesis of $m_k(t)$ begins (k=*her*1, *her*7, *deltaC*). These probabilities at a given time t are thus conditioned by the values the random variables take at an earlier time t'. Specifically the probability that the random variables take value 1 (unbound) at the time $t+\Delta t$ depends on the state of the appropriate regulatory site at time t (bound or unbound):

$$p^{rv}_{10}(t+\Delta t) = 1-P^{rv}(t+\Delta t)|[P^{rv}(t)=0], \quad \text{if the regulatory site is bound at } t,$$

$$p^{rv}_{11}(t+\Delta t) = P^{rv}(t+\Delta t)|[P^{rv}(t)=1], \quad \text{if the regulatory site is unbound at } t. \quad (5)$$

In Eqs. (5), $p^{rv}_{\alpha\beta}$ represents the probability that any random variable rv has value α at $t+\Delta t$ if it had value β at t (rv can

be $\xi_{her1/7}$, $\eta_{her1/7}$, or ξ_{deltaC} and $\alpha=1$, $\beta=0,1$), while $P^{rv}(t)$ is the probability that the regulatory site is free of repression. This probability obeys the master equation

$$dP^{rv}/dt = k_{off}^{rv}(1-P^{rv}) - k_{on}^{rv}P^{rv}. \quad (6)$$

These kinetic coefficients are discussed in [12] (Supplemental Data), where k_{on}^{rv} the rate constant for protein binding is a Michaelis-Menten function of the protein concentrations, while k_{off}^{rv} is the rate constant for dissociation of the repressor proteins from their regulatory DNA binding sites (typically biologically $k_{off}^{rv}\approx 1\ \mathrm{min}^{-1}$, implying a mean lifetime of about 1 min for the repressor bound state). The steady state of the master equation is $P^{rv}=k_{off}^{rv}/(k_{off}^{rv}+k_{on}^{rv})$. In the stochastic system transcripts are assumed to be initiated at a zero rate when the repressor is bound and at a maximal rate when it is not bound. Then to make the correspondence between the stochastic and deterministic systems, we must have $K_{her1/7}P^{her1/7}=K_{her1/7}/(1+\phi_{her1}\phi_{her7})$ and $K_{deltaC}P^{deltaC}=K_{deltaC}\phi_{deltaC}/(1+\phi_{deltaC})$, so that using the steady-state expression obtained above, $k_{on}^{\eta_{her1/7}}=k_{off}^{\eta_{her1/7}}\phi_{her1}\phi_{her7}$ and $k_{on}^{\xi_k}=k_{off}^{\xi_k}/\phi_{deltaC}$, with $\xi_k=\xi_{her1/7}$ or ξ_{deltaC}. Solving the master equation with k_{on}^{rv} previously obtained results in the forms $P^{rv}(t+\Delta t)=u^{rv}(1-\exp[-v\Delta t])+P^{rv}(t)\exp[-v^{rv}\Delta t]$, where $v^{rv}=(k_{off}^{rv}+k_{on}^{rv})$ and $u^{rv}=k_{off}^{rv}/v^{rv}$. Inserting these solutions into Eq. (5) one obtains

$$p_{10}^{rv}(t+\Delta t) = u^{rv}(1-e^{[-v^{rv}\Delta t]}),$$

if the regulatory site is bound at t,

$$p_{11}^{rv}(t+\Delta t) = u^{rv}(1-e^{[-v^{rv}\Delta t]}) + e^{[-v^{rv}\Delta t]},$$

if the regulatory site is unbound at t, (7)

where $rv=\xi_{her1/7}$, $\eta_{her1/7}$ or ξ_{deltaC}.

Following the same procedure, the probability that the random variables (rv) take value 0 at the time $t+\Delta t$ is given by

$$p_{01}^{rv}(t+\Delta t) = (1-u^{rv})(1-e^{[-v^{rv}\Delta t]}),$$

if the regulatory site is unbound at t,

$$p_{00}^{rv}(t+\Delta t) = 1-u^{rv}(1-e^{[-v^{rv}\Delta t]}),$$

if the regulatory site is bound at t. (8)

The temporal evolution of p_k and m_k for the cells of the linear array are calculated with Eqs. (1), while the function f_k that represents the rate of production of new mRNA molecules m_k is given by Eqs. (4). The random variables $\xi_{her1/7}$, $\eta_{her1/7}$, and ξ_{deltaC} are obtained through Eqs. (7) and (8). The simulations are performed as in the deterministic model (detailed in Sec. II): we begin with the linear array of N_{start} cells and integrate Eqs. (1), and the growth of the PSM is assumed to be produced by mitosis experienced by the last cells at the posterior end of the linear array. The wave-front velocity is given by the PSM growth rate of one cell every 5 min. We assume that the wave front interacts with cells by stopping the oscillations. The system with noise tends to the deterministic system in the limit of large k_{off}^{rv} [i.e., $\langle \xi_{her1/7,deltaC}\rangle_{k_{off}^{\xi}\to\infty}=1/(1+\phi_{her1}\phi_{her7})$, $\langle \eta_{her1/7}\rangle_{k_{off}^{\eta}\to\infty}=\phi_{deltaC}/(1+\phi_{deltaC})$]. In Fig. 5, the concentration of m_{her1} versus time calculated using the deterministic model (detailed in Sec. II) and the model with noise for a typically biologic noise level ($k_{off}^{\xi_{her1/7}}=k_{off}^{\eta_{her1/7}}=k_{off}^{\xi_{deltaC}}=1$) and for a higher noise level ($k_{off}^{\xi_{her1/7}}=k_{off}^{\eta_{her1/7}}=k_{off}^{\xi_{deltaC}}=0.1$) are compared. A random variability in the amplitude and shape of individual oscillation peaks can be seen for both results obtained with noise. In addition, as the amplitude of noise increases, the oscillations of m_{her1} are not in phase with the deterministic model oscillations. Nevertheless, the oscillations are practically synchronized between the deterministic and the typically biologic noise level. These results are in good agreement with those of [12].

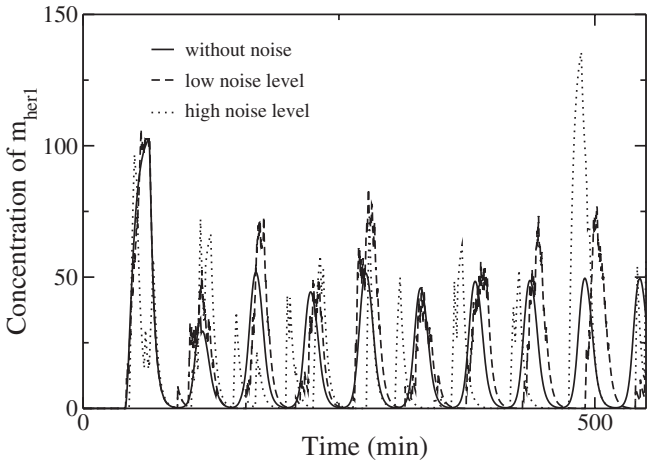

FIG. 5. Concentration of messenger RNA molecules (number of molecules per cell) of gene *her*1 as a function of time for any cell of the linear array. Comparison of results obtained using the deterministic one-dimensional model described in Sec. II (solid line) and the stochastic model for a typically biologically noise level (dashed line, $k_{off}^{\xi_{her1/7}}=k_{off}^{\eta_{her1/7}}=k_{off}^{\xi_{deltaC}}=1$) and for a higher noise level (dotted line, $k_{off}^{\xi_{her1/7}}=k_{off}^{\eta_{her1/7}}=k_{off}^{\xi_{deltaC}}=0.1$). The parameter values are $a=4.5$, $b=0.23$, $c=0.23$, $K_k=33$, $p_{her1/7}^{crit}=40$, $p_{delta}^{crit}=1000$, $T_{m_{her1}}=20.5$, $T_{m_{her7}}=15$, $T_{m_{deltaC}}=16$, $T_{p_{her1}}=2.8$, $T_{p_{her7}}=1.7$, and $T_{p_{deltaC}}=20$ min. The concentrations of protein and message molecules have the same behavior as the concentration of m_{her1} shown in this figure.

Finally, a somite pattern for the stochastic model is shown in Fig. 6. The wave front advances at a speed of 5 min per cell, freezing the oscillations of protein and mRNA concentrations.

V. PERTURBATION OF THE SOMITOGENESIS WAVE FRONT

Finally perturbations in Fgf8 concentration are simulated as transient manipulation of the wave front and their consequences on the size of the somites are analyzed. An experimental prediction related to delay times dependence of our model is proposed.

The concentration of Fgf8 signaling is high in the caudal PSM and drops between the intermediate and the rostral PSM as indicated by the top part of the Fig. 1. In this paper we assume that somite formation can begin when the Fgf8 signaling falls below a critical level and this level moves

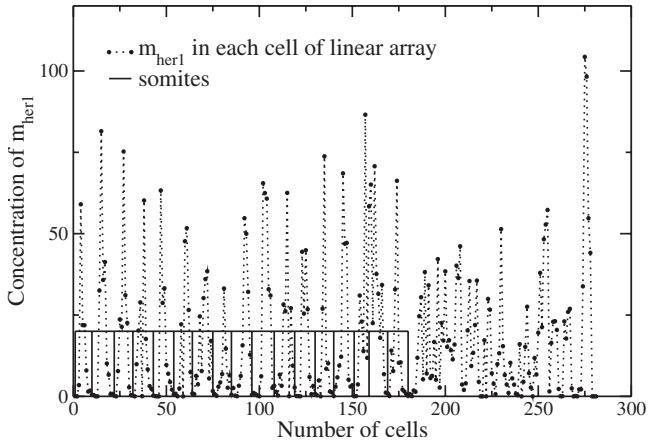

FIG. 6. Concentration of messenger molecules (number of molecules per cell) of gene *her*1 as a function of the number of cell at the linear array. The concentrations were calculated using the stochastic model for haploid cells with a noise level given by $k_{off}^{\xi_{her1/7}}=k_{off}^{\eta_{her1/7}}=k_{off}^{\xi_{deltaC}}=1$ and assuming the rest of the parameters equal to the used ones in Fig. 5. The wave front advances at a speed of 5 min by cell and the initial PSM is of 100 cells. Somites obtained in the simulation at $t=900$ min are shown here. All the other concentrations of protein and message molecules in the cells (i.e., p_k with $k=her1$, *her*7, *deltaC* and m_k with $k=her7$, *deltaC*) have similar behavior as the concentration of m_{her1}.

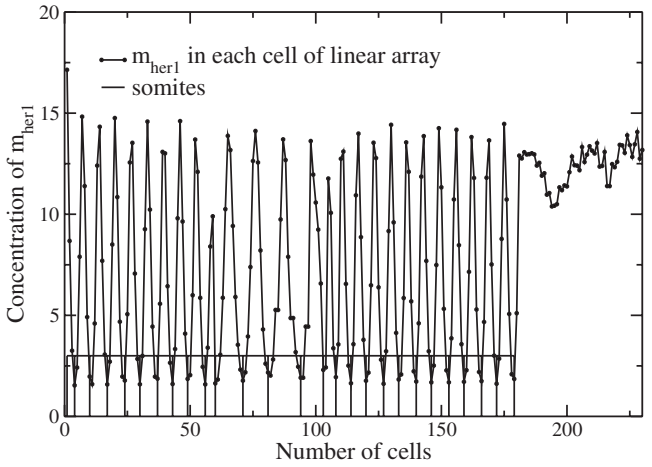

FIG. 7. Concentration of gene *her*1 mRNA (number of molecules per cell) as a function of the number of cell in the linear array. The concentrations were calculated using the deterministic version of the one-dimensional model and assuming the same parameter values as in Figs. 2 (see caption) and 3. The wave front advances at velocity of 5 min per cell, but between cells 60 and 100 there is a perturbation in the Fgf8 levels, resulting in a change in the wave-front velocity: the velocity increases to 3 min per cell. The patterns of somites are altered by the perturbations (see Fig. 3).

towards the caudal end of the PSM with a constant velocity. Now it is known that a transient manipulation of the wave front in zebrafish embryos alters the size of the somites [35]: smaller somites result when there is transient inhibition of Fgf8 signaling, whereas larger somites result in the presence of transient activation. Chemical inhibitor and transplantation of Fgf8 beads are used for altering the level of Fgf8 signaling that regulates the position of the wave front within the PSM [11,40]. The alteration of Fgf8 level is present in a reduced PSM zone and is independent of the growth of the caudal region.

Assuming that such perturbations in Fgf8 concentration directly result in changes in the wave-front velocity, we will modify the wave-front velocity in our model and analyze their consequences. The perturbed pattern of the resulting somites depends on how the wave-front velocity changes. In Fig. 7 an example of such perturbations is shown that has been obtained with the deterministic one-dimensional model by altering the wave-front velocity. The other parameters in the model required for finding the protein and mRNA concentrations are the same as in Fig. 3. Specifically, as in the unperturbed system, the wave front initially advances a rate of 5 min per cell, but between cells 60 and 100 the wave front is perturbed. The velocity is increased to 3 min per cell in the cell interval (60, 100) and larger somites are formed (see Fig. 7) in comparison with the results of Fig. 3. On the other hand, when the velocity is decreased in a group of cells smaller somites are formed. In general, alterations of the wave-front velocity perturb the resulting somite pattern in a grossly irregular manner. Similar results were recently obtained with a mathematical formulation of another version of the clock and wave-front model by Baker, Schnell, and Maini [4,13].

In order to test the validity of our model, we propose to perturb somitic pattern altering the segmentation clock period. The oscillation period depends on the FGF8 concentration level [41] because the cells located at the region of high FGF8 concentration display period oscillations longer than those of low FGF8 concentration in order that the cells in the anterior region of the PSM slow down and finally cease their oscillations as they emerge from the PSM and begin differentiation. The alteration of the segmentation clock period might then be possible in an experiment by modifying the FGF8 concentration level on the whole extent of the PSM. According to the assumption of our model FGF8 concentration variation has an effect only on *her*1/7 messengers and proteins. If the delay times associated with *her*1/7 messengers and proteins are reduced, the number of somites increases, while the average somite size decreases. This behavior is produced by decreasing the delay time associated with *her*1/7 messengers and proteins until a given threshold in which the temporal oscillations are lost and correspondingly the somitic pattern disappears [12]. This is an experimental prediction related to delay times dependence of our model that can be used in some future experiment to test its validity.

VI. CONCLUSIONS

In this paper we introduce an extension of the "delay model" for the genetic network associated with zebrafish somitogenesis [12] by taking into account the interaction of the oscillation clock with the determination front to obtain a growing approximately spatially periodic sequence of somites for the zebrafish embryo. The determination front represents the position at which the FGF8 concentration

gradient falls below a critical value. We assume that the Fgf8 concentration acts as a morphogen creating an intracellular signalling cascade that ultimately controls transcription and translation of the gene products. As a first approximation, we simply propose that the Fgf8 concentration level acts as an on-off switch by stopping the gene oscillations (Fig. 3). In order to consider a genetic network related explanation for the on-off switching we use that a Hes6-related hairy/Enhancer of split-related gene, *her*13.2, links FGF signaling to the Notch-regulated oscillation machinery in zebrafish to include an additional term to enhance the self-repression of *her*1 through formation of Her1-Her13.2 heterodimer complex [38]. The condition of stopping gene oscillations is used to calculate the Her13.2 protein concentration, which is high in posterior PSM and drops in anterior PSM agreeing with the experimental results (Fig. 4).

On the other hand, we also consider the consequences that gene regulation is in reality a noisy process which is likely to be crucial in a real developmental situation because of the small number of intracellular molecules involved. The presomitic pattern obtained with a typical noise level is qualitatively the same that the deterministic one (Fig. 6).

We simulated the transient manipulation of the wave front in zebrafish embryos [35]. Larger somites are formed when the wave-front velocity is locally increased, whereas smaller somites result if there is a local decrease in the wave-front velocity (Fig. 7). We propose another way to perturb the presomitic pattern by changing the segmentation clock period. When *her*1/*her*7 messengers and proteins delay times are reduced, the number of somites increases, while the average somite size decreases. This an experimental prediction of our model that can be used in some future experiment to test its validity.

[1] I. Palmeirim, D. Henrique, D. Ish-Horowicz, and O. Pourquié, Cell **91**, 639 (1997).
[2] J. Cooke and E. C. Zeeman, J. Theor. Biol. **58**(2), 455 (1976).
[3] O. Pourquié, Science **301**, 328 (2003).
[4] R. E. Baker, S. Schnell, and P. K. Maini, Dev. Biol. **293**, 116 (2006).
[5] A. Aulhela and O. Pourquié (unpublished).
[6] A. Aulhela and B. G. Herrmann, Genes Dev. **18**, 2060 (2004).
[7] P. C. G. Rida, N. L. Minh, and Y. Jiang, Dev. Biol. **265**, 2 (2004).
[8] H. Meinhardt, *Models of Biological Pattern Formation* (Academic Press, London, 1982); *Models of Segmentation*, Vol. 118 of *Somites in Developing Embryos*: NATO Advanced Study Institute, Series A (Plenum Press, New York, 1986).
[9] D. R. N. Primmett, W. E. Norris, G. J. Carlson, R. J. Keynes, and C. D. Stern, Development **105**, 119 (1989); D. R. N. Primmett, C. D. Stern, and R. J. Keynes, *ibid.* **104**, 331 (1988); C. D. Stern, S. E. Fraser, R. J. Keynes, and D. R. N. Primmett, *ibid.* **104S**, 231 (1988).
[10] K. J. Dale and O. Pourquié, BioEssays **22**, 72 (2000).
[11] J. Dubrulle, M. J. McGrew, and O. Pourquié, Cell **106**, 219 (2001).
[12] J. Lewis, Curr. Biol. **13**, 1398 (2003).
[13] R. E. Baker, S. Schnell, and P. K. Maini, J. Math. Biol. **52**, 458 (2006).
[14] O. Pourquié, Int. J. Dev. Biol. **47**, 597 (2003).
[15] A. Goldbeter and O. Pourquié, J. Theor. Biol. **252**, 574 (2008).
[16] P. Francois and V. Hakim, Phys. Rev. E **72**, 031908 (2005).
[17] A. S. Ribeiro, Phys. Rev. E **75**, 061903 (2007).
[18] E. Ullner, A. Zaikin, E. I. Volkov, and J. García-Ojalvo, Phys. Rev. Lett. **99**, 148103 (2007).
[19] L. G. Morelli and F. Jülicher, Phys. Rev. Lett. **98**, 228101 (2007).
[20] L. Glass and M. C. Mackey, *From Clocks to Chaos: The Rhythms of Life* (Princeton University Press, Princeton, 1988).
[21] M. B. Elowitz and S. Leibler, Nature (London) **403**, 335 (2000).
[22] C. Freitas, S. Rodrigues, J. Charrier, M. Teillet, and I. Palmeirim, Development **128**, 5139 (2001).
[23] A. C. Oates and R. K. Ho, Development **129**, 2929 (2002).
[24] M. K. Henry, K. K. Urban, J. P. Dill, M. F. Merlie, Page, C. B. Kimmel, and S. L. Amacher, Development **129**, 3693 (2002).
[25] K. Horikawa (private communication).
[26] F. Giudicelli, E. M. Özbudak, G. J. Wright, and J. Lewis, PLoS Biol. **5**, 1309 (2007).
[27] M. Gajewski, D. Sieger, B. Alt, C. Leve, S. Hans, C. Wolff, B. K. Rohr, and D. Tautz, Development **130**, 4269 (2003).
[28] U. Alon, *An Introduction to Systems Biology, Design Principles of Biological Circuits* (Mathematical & Computational Biology, 2006).
[29] B. Alberts, A. Johnson, J. Lewis, M. Raff, K. Roberts, and P. Walter, *Molecular Biology of the Cell* (Garland Science, New York, 2002).
[30] M. H. Glickman and A. Ciechanover, Physiol. Rev. **82**, 373 (2002).
[31] Y. Wang, C. L. Liu, J. D. Storey, R. J. Tibshirani, D. Herschlag, and P. O. Brown, Proc. Natl. Acad. Sci. U.S.A. **99**, 5860 (2002).
[32] O. Cinquin, PLOS Comput. Biol. **3**, 0293 (2007).
[33] D. M. Prescott and M. A. Bender, Exp. Cell Res. **26**, 260 (1962).
[34] H. Horikawa, H. K. Ishimatsu, E. Yoshimoto, S. Kondo, and H. Takeda, Nature (London) **441**, 719 (2006).
[35] S. A. Holley and H. Takeda, PLOS Comput. Biol. **13**, 481 (2002).
[36] Y. J. Jiang, B. L. Aerne, L. Smithers, C. Haddon, D. I. Horowicz, and J. Lewis, Nature (London) **408**, 475 (2000).
[37] A. Kawamura, S. Koshida, H. Hijikata, T. Sakaguchi, H. Kondoh, and S. Takada, Genes Dev. **19**, 1156 (2005).
[38] A. Kawamura, S. Koshida, H. Hijikata, T. Sakaguchi, H. Kondoh, and S. Takada, Genes Dev. **19**, 1156 (2005).
[39] P. S. Swain, M. B. Elowitz, and E. D. Siggia, Proc. Natl. Acad. Sci. U.S.A. **99**, 12795 (2002).
[40] A. Sawada, M. Shinya, Y. J. Jiang, A. Kawakami, A. Kuroiwa, and H. Takeda, Development **128**, 4873 (2001).
[41] F. Giudicelli, E. M. Özbudak, G. J. Wright, and J. Lewis, PLOS Comput. Biol. **5**, 1309 (2007).